Available online at www.sciencedirect.com

ScienceDirect

Mathematics and Computers in Simulation 79 (2008) 700–715

MATHEMATICS AND COMPUTERS IN SIMULATION

www.elsevier.com/locate/matcom

# A numerical method for solution of the two-dimensional sine-Gordon equation using the radial basis functions

Mehdi Dehghan*, Ali Shokri

*Department of Applied Mathematics, Faculty of Mathematics and Computer Science, Amirkabir University of Technology, No. 424, Hafez Avenue, Tehran, Iran*

Received 8 August 2007; received in revised form 24 April 2008; accepted 27 April 2008
Available online 15 May 2008

**Abstract**

The nonlinear sine-Gordon equation arises in various problems in science and engineering. In this paper, we propose a numerical scheme to solve the two-dimensional damped/undamped sine-Gordon equation. The proposed scheme is based on using collocation points and approximating the solution employing the thin plate splines (TPS) radial basis function (RBF). The new scheme works in a similar fashion as finite difference methods. Numerical results are obtained for various cases involving line and ring solitons.


*Keywords:* Two-dimensional damped/undamped sine-Gordon equation; Soliton; Collocation; Radial basis function (RBF); Thin plate splines (TPS)

## 1. Introduction

This paper is devoted to the numerical computation of the two-dimensional time-dependent nonlinear sine-Gordon equation. The two-dimensional sine-Gordon equation is given by

$$\frac{\partial^2 u}{\partial t^2} + \beta\frac{\partial u}{\partial t} = \frac{\partial^2 u}{\partial x^2} + \frac{\partial^2 u}{\partial y^2} + \phi(x, y)\sin(u), \tag{1.1}$$

in some continuous domain with suitable initial and Neumann's boundary conditions. The parameter $\beta$ is the so-called *dissipative* term, which is assumed to be a real number with $\beta \geq 0$. When $\beta = 0$, Eq. (1.1) reduces to the undamped sine-Gordon equation in two space variables, while when $\beta > 0$, to the damped one.

In recent years, some attention has also been paid to models which possess soliton-like structures in higher dimensions [14]. In particular, the Josephson junction model [23] which consists of two layers of super conducting material separated by an isolating barrier. This model is found to have many applications in electronics and can be described by the two-dimensional undamped sine-Gordon equation. Moreover, it is found to possess soliton-like solutions [9].

As said in [3], solitons represent essentially special wave-like solutions to nonlinear dynamic equations. In fact these waves progress through the medium without experiencing any deformation due to dispersion. Moreover no deformation

* Corresponding author. Tel.: +98 21 64542503; fax: +98 21 66497930.
*E-mail addresses:* mdehghan@aut.ac.ir (M. Dehghan), shokri.a@gmail.com (A. Shokri).

0378-4754/$32.00 © 2008 IMACS. Published by Elsevier B.V. All rights reserved.
doi:10.1016/j.matcom.2008.04.018

occurs after interaction with other solitons. Solitons have been shown to play a central role in the theory of nonlinear differential equations. Soliton solutions have been found for a variety of equations, including the Korteweg–de Vries equation, the nonlinear Schrödinger equation and the sine-Gordon equation [3]. Physical applications where solitons have been shown to emerge abound, they include condensed-matter physics, shallow-water waves, optical fibres and Josephson-junction oscillators, among others [27]. They may be considered as fundamental excitations of a certain class of fully integrable Hamiltonian systems modeled by nonlinear dispersive partial differential equations of evolution. They appear as special solitary waves, essentially nondissipative localized packets of energy (either coherent pulses, kinks or envelopes) and, in some manner, behave like particles. The underlying partial differential equations can be obtained for a variety of time and space scales in many types of weakly nonlinear, dispersive systems and, therefore, the ubiquitousness of soliton solutions in many physical areas (classical fluid dynamics, plasma physics, fibre optics, dislocation theory and Josephson physics) will not surprise a physicist (see [3] and references therein).

The review paper [20] gives an extensive overview of the soliton solutions for some well-known partial differential equations such as KdV, mKdV, sine-Gordon, and nonlinear Schrödinger equations. Different analytical methods of treatment as well as those of numerical techniques are presented in this paper. As is said in [20] solitons are a special kind of localized wave, essentially of nonlinear kind. For further details, the reader refers to Ref. [20] which is an overview of the theory of solitons and its applications.

As is said in [14] analytical solutions to the unperturbed sine-Gordon equation with zero damping in higher dimensions have been obtained [14] by Hirota, Lamb's method, Bäcklund transformation and Painlevè transcendents, while approximate solutions, chronogically, include those obtained by Christiansen and Lomdahl [9](see [14] and references therein).

As is said in [3] although models that can be solved exactly are important because they display clearly the effect of the basic elements in play (e.g., special symmetries), they are often only idealizations of more realistic physical systems. In fact, in reality the presence of dissipative effects, impurities, and imperfections in the boundaries and other small perturbations can never be avoided and lead to equations too complicated to be integrated exactly. Furthermore, in more realistic systems including, for example, damping effects of external forcing, analytical solutions are no longer possible and numerical methods must be used. The same is true for solitons or soliton-like structures in two or three spatial dimensions, where the properties of the solitary waves depend essentially on the number of space dimensions [3]. This remark is of interest because there may be a mutual stimulation of careful numerical studies and theoretical work. A classical example is the investigation of Zabusky and Kruskal who coined the word soliton in 1965 for a certain class of solitary waves pulses that they obtained from a numerical investigation of the Korteweg–de Vries equation.

Great number of publications are concerned with the numerical solution of one-dimensional solitons, including finite differences as well as finite element methods (see, for example, the list of references in [2]).

As is said in [4] for the undamped SG equation in higher dimensions exact solutions have been obtained in [21] using Hirotas method, in [37] using Lamb's method, in [10] by Balcklund transformation and in [24] by Painleve transcendents.

Numerical solutions for two-dimensional undamped sine-Gordon equation, have been given among others by Guo et al. [18] using two finite difference schemes, Xin [36] who studied sine-Gordon equation as an asymptotic reduction of the two level dissipationless Maxwell–Bloch system, Christiansen and Lomdahl [9] using a generalized leapfrog method and Argyris et al. [3] with finite-elements where both methods using appropriate initial conditions have been successfully applied with the latter one giving slightly better results, Sheng et al. [33] with a split cosine scheme, Bratsos [6] using a three-time level fourth-order explicit finite-difference scheme, etc. Numerical approaches to the damped sine-Gordon equation can also be found in Nakajima et al. [31] who consider dimensionless loss factors and unitless normalized bias, Gorria et al. [17] who studied the nonlinear wave propagation in a planar wave guide consisting of two rectangular regions joined by a bent of constant curvature using as a model the kink solutions of the sine-Gordon equation, where this can be considered as a part of similar works examining the effect of the curvature on analogous nonlinear physical phenomena (see, for example, the list of references in [5,7]), Bratsos [6], Bratsos and Djidjeli et al. [14] where the method arises from a two-step one-parameter leapfrog scheme, which is a generalization to that used by Christiansen and Lomdahl [9], etc. Recently authors of [13] developed the dual reciprocity boundary element method for solving the two-dimensional damped and undamped sine-Gordon equations.

In this paper, we will concentrate on the numerical solution of the two-dimensional sine-Gordon equation using radial basis functions (RBF) as a truly meshless/meshfree method.

### 1.1. Radial basis function approximation

A meshfree method does not require a mesh to discretize the domain of the problem under consideration, and the approximate solution is constructed entirely based on a set of scattered nodes. Several domain type meshfree methods such as elementfree Galerkin method, reproducing kernel particle method, the point interpolation method and the meshless Petrov-Galerkin method have been proposed and achieved remarkable progress in solving a wide range of static and dynamic problems for solid and structures (see, for example, [1] and references therein).

Radial basis function (RBF) is one of the most recently developed meshless methods that has attracted attention in recent years, especially in the area of computational mechanics [8,34,28]. This method does not require mesh generation which makes them advantageous for 3D problems as well as problems that require frequent re-meshing such as those arising in nonlinear analysis. Due to its simplicity to implement, it represents an attractive alternative to the finite-difference [11,39–41] method (FDM), the finite-element method (FEM) and the boundary-element method (BEM) as a solution method of nonlinear differential equations. However, it is only since rather recently that RBF has been used to approximate solutions for partial differential equations and therefore this area is still relatively unexplored. The roots of RBF goes back to the early 1970s, when it was used for fitting scattered data [19]. In 1982, Nardini and Brebbia [32] coupled RBF with BEM in a technique called dual-reciprocity BEM to solve free-vibration problems, where the RBF was used to transform the domain integrals into boundary integrals. Thereafter, many researchers have used RBF in conjunction with BEM to solve various problems in computational mechanics. The method, however has not been applied directly to solve partial differential equations until 1990 by Kansa [25,26]. Since then, many researchers have suggested several variations to the original method (see, for example, [12] and references therein). In general, the RBF method expands the solution of a problem in terms of RBFs and chooses expansion coefficients such that the governing equations and boundary conditions are satisfied at some selected domain and boundary points. However, one of the important issues in applying this technique is the determination of the proper form of RBF for a given differential equation.

Most of the available RBFs involve a parameter, called shape factor (such as multiquadric (MQ), inverse multiquadric (IMQ), Gaussian, etc.) which needs to be selected so that the required accuracy of the solution is attained.

The traditional RBFs are globally defined functions which result in a full resultant coefficient matrix. This hinders the application of the RBFs to solve large-scale problems due to severe ill-conditioning of the coefficient matrix. To tackle this ill-conditioning problem, a new class of compactly supported RBFs constructed by [35]. For the theoretical developments of the RBFs in scattered data interpolation, Madych and Nelson [29,30] showed that the RBF-MQ interpolant employs exponential convergence with minimal semi-norm errors. Recently, Franke and Schaback [15,16] provided a theoretical proof in using the RBFs for the numerical solution of PDEs. More recently, Hon and Wu [22] gave a theoretical justification in combining the RBFs with those advanced techniques of domain decomposition, multilevel/multigrid, Schwarz iterative schemes, and preconditioning in the FEM discipline.

The approximation of a distribution $u(\mathbf{x})$, using radial basis functions, may be written as a linear combination of $N$ radial functions; usually it takes the following form:

$$u(\mathbf{x}) \simeq \sum_{j=1}^{N} \lambda_j \varphi(\mathbf{x}, \mathbf{x}_j) + \psi(\mathbf{x}), \quad \text{for } \mathbf{x} \in \Omega \subset \mathbb{R}^d, \tag{1.2}$$

where $N$ is the number of data points, $\mathbf{x} = (x_1, x_2, \ldots, x_d)$, $d$ is the dimension of the problem, $\lambda$'s are coefficients to be determined and $\varphi$ is the radial basis function. Eq. (1.2) can be written without the additional polynomial $\psi$. In that case $\varphi$ must be *unconditionally positive definite* to guarantee the solvability of the resulting system (e.g. Gaussian or inverse multiquadrics). However, $\psi$ is usually required when $\varphi$ is *conditionally positive definite*, i.e., when $\varphi$ has a polynomial growth towards infinity. Examples are thin plate splines and multiquadrics. We will use the thin plate splines for the new numerical scheme introduced in Section 2. The generalized thin plate splines (TPS) defined as:

$$\varphi(\mathbf{x}, \mathbf{x}_j) = \varphi(r_j) = r_j^{2m} \log(r_j), \quad m = 1, 2, 3, \ldots, \tag{1.3}$$

where $r_j = \|\mathbf{x} - \mathbf{x}_j\|$ is the Euclidean norm.

Since $\varphi$ in (1.3) is $C^{2m-1}$ continuous, so higher order thin plate splines must be used for higher order partial differential operators. For the nonlinear sine-Gordon equation, an $m = 2$ is used for thin plate splines (i.e. second order thin plate splines).

If $\mathcal{P}_q^d$ denotes the space of $d$-variate polynomials of order not exceeding $q$, and letting the polynomials $P_1, \ldots, P_m$ be the basis of $\mathcal{P}_q^d$ in $\mathbb{R}^d$, then the polynomial $\psi(\mathbf{x})$, in Eq. (1.2), is usually written in the following form:

$$\psi(\mathbf{x}) = \sum_{i=1}^{m} \zeta_i P_i(\mathbf{x}), \tag{1.4}$$

where $m = (q-1+d)!/(d!(q-1)!)$.

To determine the coefficients $(\lambda_1, \ldots, \lambda_N)$ and $(\zeta_1, \ldots, \zeta_m)$, the collocation method is used. However, in addition to the $N$ equations resulting from collocating (1.2) at the $N$ points, an extra $m$ equations are required. This is insured by the $m$ conditions for (1.2),

$$\sum_{j=1}^{N} \lambda_j P_i(\mathbf{x}_j) = 0, \quad i = 1, \ldots, m. \tag{1.5}$$

In a similar representation as (1.2), for any linear partial differential operator $\mathcal{L}$, $\mathcal{L}u$ can be approximated by

$$\mathcal{L}u(\mathbf{x}) \simeq \sum_{j=1}^{N} \lambda_j \mathcal{L}\varphi(\mathbf{x}, \mathbf{x}_j) + \mathcal{L}\psi(\mathbf{x}). \tag{1.6}$$

The layout of the rest of this paper is as follows: In Section 2 we apply the method on the two-dimensional sine-Gordon equation. The results of numerical experiments are presented in Section 3. Section 4 is dedicated to a brief conclusion. Finally some references are introduced at the end.

## 2. Implementation of the numerical method

Consider the two-dimensional sine-Gordon equation

$$\frac{\partial^2 u}{\partial t^2} + \beta \frac{\partial u}{\partial t} = \frac{\partial^2 u}{\partial x^2} + \frac{\partial^2 u}{\partial y^2} + \phi(x, y)\sin(u), \tag{2.1}$$

with $u(x, y, t)$ in the region $\Omega = \{(x, y), L_x^0 < x < L_x^1, L_y^0 < y < L_y^1\}$ for $t > 0$ and $u$ a sufficiently differentiable function.

Initial conditions associated with Eq. (2.1) will be assumed to be of the form

$$u(x, y, 0) = f(x, y), \quad L_x^0 < x < L_x^1, \quad L_y^0 < y < L_y^1, \tag{2.2}$$

with initial velocity

$$\frac{\partial u}{\partial t}(x, y, t) = g(x, y), \quad \text{for } t = 0, L_x^0 < x < L_x^1, L_y^0 < y < L_y^1. \tag{2.3}$$

In Eq. (2.1) the function $\phi(x, y)$ may be interpreted as the Josephson current density, while in Eqs. (2.2)–(2.3) the functions $f(x, y)$ and $g(x, y)$ represent wave modes or kinks and velocity, respectively. In the experiments the kink profiles will be considered known from the relevant one-dimensional problem. They will operate across lines or closed curves in the $xy$-plane. These curves will be called line and ring soliton waves, respectively.

Boundary conditions will be assumed to be of the form

$$\frac{\partial u}{\partial x}(x, y, t) = p(x, y, t), \quad \text{for } x = L_x^0 \text{ and } x = L_x^1, L_y^0 < y < L_y^1, t > 0, \tag{2.4}$$

and

$$\frac{\partial u}{\partial y}(x, y, t) = q(x, y, t), \quad \text{for } y = L_y^0 \text{ and } y = L_y^1, L_x^0 < x < L_x^1, t > 0, \tag{2.5}$$

where $p(x, y, t)$ and $q(x, y, t)$ are normal gradients along the boundary of the region $\Omega$. Some exact solutions of the undamped sine-Gordon equation have been obtained (see [14] and references therein) but not to the damped sine-Gordon equation.

First, let us discretize (2.1) according to the following $\theta$-weighted scheme

$$\frac{u(x,y,t+\delta t)-2u(x,y,t)+u(x,y,t-\delta t)}{(\delta t)^2}+\beta\frac{u(x,y,t+\delta t)-u(x,y,t-\delta t)}{2\delta t}$$
$$=\theta\nabla^2 u(x,y,t+\delta t)+(1-\theta)\nabla^2 u(x,y,t)+\phi(x,y)\sin(u(x,y,t)), \tag{2.6}$$

where $\nabla$ is the gradient differential operator, $0\le\theta\le 1$, and $\delta t$ is the time step size.

Rearranging (2.6), using the notation $u^n=u(x,y,t^n)=u^n(x,y)$ where $t^n=t^{n-1}+\delta t$, we obtain

$$\left(1+\frac{\beta\delta t}{2}\right)u^{n+1}-\theta(\delta t)^2\nabla^2u^{n+1}=2u^n+(1-\theta)(\delta t)^2\nabla^2u^n-\left(1-\frac{\beta\delta t}{2}\right)u^{n-1}+(\delta t)^2\phi(x,y)\sin(u^n). \tag{2.7}$$

Assuming that there are a total of $(N-3)$ interpolation points, $u(x,y,t^n)$ can be approximated by

$$u^n(x,y)\simeq\sum_{j=1}^{N-3}\lambda_j^n\varphi(r_j)+\lambda_{N-2}^n x+\lambda_{N-1}^n y+\lambda_N^n. \tag{2.8}$$

To determine the interpolation coefficients $(\lambda_1,\lambda_2,\ldots,\lambda_{N-2},\lambda_{N-1},\lambda_N)$, the collocation method is used by applying (2.8) at every point $(x_i,y_i)$, $i=1,2,\ldots,N-3$. Thus we have

$$u^n(x_i,y_i)\simeq\sum_{j=1}^{N-3}\lambda_j^n\varphi(r_{ij})+\lambda_{N-2}^n x_i+\lambda_{N-1}^n y_i+\lambda_N^n, \tag{2.9}$$

where $r_{ij}=\sqrt{(x_i-x_j)^2+(y_i-y_j)^2}$. The additional conditions due to (1.5) are written as

$$\sum_{j=1}^{N-3}\lambda_j^n=\sum_{j=1}^{N-3}\lambda_j^n x_j=\sum_{j=1}^{N-3}\lambda_j^n y_j=0. \tag{2.10}$$

Writing (2.9) together with (2.10) in a matrix form we have

$$[u]^n=\mathbf{A}[\lambda]^n, \tag{2.11}$$

where $[u]^n=[u_1^n u_2^n\ldots u_{N-3}^n 0\,0\,0]^{\mathrm{T}}$, $[\lambda]^n=[\lambda_1^n\,\lambda_2^n\ldots\lambda_N^n]^{\mathrm{T}}$ and $\mathbf{A}=[a_{ij},1\le i,j\le N]$ is given by

$$\mathbf{A}=\begin{bmatrix}\varphi_{11} & \cdots & \varphi_{1(N-3)} & x_1 & y_1 & 1\\ \vdots & \ddots & \vdots & \vdots & \vdots & \vdots\\ \varphi_{(N-3)1} & \cdots & \varphi_{(N-3)(N-3)} & x_{N-3} & y_{N-3} & 1\\ x_1 & \cdots & x_{N-3} & 0 & 0 & 0\\ y_1 & \cdots & y_{N-3} & 0 & 0 & 0\\ 1 & \cdots & 1 & 0 & 0 & 0\end{bmatrix}. \tag{2.12}$$

Assuming that there are $k<(N-3)$ internal points and $(N-3-k)$ boundary points, then the $(N\times N)$ matrix $\mathbf{A}$ can be split into: $\mathbf{A}=\mathbf{A}_d+\mathbf{A}_b+\mathbf{A}_e$, where

$$\begin{aligned}&\mathbf{A}_d=[a_{ij}\text{ for }(1\le i\le k,\ 1\le j\le N)\text{ and 0 elsewhere}],\\&\mathbf{A}_b=[a_{ij}\text{ for }(k+1\le i\le N-3,\ 1\le j\le N)\text{ and 0 elsewhere}],\\&\mathbf{A}_e=[a_{ij}\text{ for }(N-2\le i\le N,\ 1\le j\le N)\text{ and 0 elsewhere}].\end{aligned} \tag{2.13}$$

Using the notation $\mathcal{L}\mathbf{A}$ to designate the matrix of the same dimension as $\mathbf{A}$ and containing the elements $\tilde a_{ij}$, where $\tilde a_{ij}=\mathcal{L}a_{ij}$, $1\le i,j\le N$, then Eq. (2.7) together with (2.4)–(2.5) can be written, in the matrix form, as

$$B[\lambda]^{n+1}=C[\lambda]^n-\left(1-\frac{\beta\delta t}{2}\right)[u_d]^{n-1}+(\delta t)^2[\phi S]^n+[H]^{n+1}, \tag{2.14}$$

where

$$B = \left(1 + \frac{\beta\delta t}{2}\right) A_d - \theta(\delta t)^2 \nabla^2 A_d + \nabla A_b + A_e,$$
$$C = 2A_d + (1-\theta)(\delta t)^2 \nabla^2 A_d,$$
$$[u_d]^n = [u_1^n \ldots u_k^n 0 \ldots 0]^{\mathrm{T}},$$
$$[\phi S]^n = [\phi_1 \sin(u_1^n) \ldots \phi_k \sin(u_k^n) 0 \ldots 0]^{\mathrm{T}},$$

and $[H]^{n+1} = [0 \ldots 0 h_{k+1}^{n+1} \ldots h_{N-3}^{n+1} 0\,0\,0]^{\mathrm{T}}$ (respect to the boundary condition, $h = p$ or $q$). Eq. (2.14) is obtained by combining (2.7), which applies to the domain points, while (2.4)–(2.5) apply to the boundary points.

At $n = 0$ the Eq. (2.14) has the following form:

$$B[\lambda]^1 = C[\lambda]^0 - \left(1 - \frac{\beta\delta t}{2}\right)[u_d]^{-1} + (\delta t)^2[\phi S]^0 + [H]^1. \tag{2.15}$$

To approximate $u^{-1}(x, y)$ in the internal points the initial velocity used. For this we discretize the initial velocity as

$$\frac{u^1(x, y) - u^{-1}(x, y)}{2\delta t} = g(x, y). \tag{2.16}$$

Writing (2.15) together with (2.16) we have

$$\left\{B + \left(1 - \frac{\beta\delta t}{2}\right) A_d\right\}[\lambda]^1 = C[\lambda]^0 + 2\left(1 - \frac{\beta\delta t}{2}\right)\delta t[G] + (\delta t)^2[\phi S]^0 + [H]^1, \tag{2.17}$$

where $[G] = [g_1 \ldots g_k\, 0 \ldots 0]^{\mathrm{T}}$.

Since the coefficient matrix is unchanged in time steps, we use the LU factorization to the coefficient matrix only once and use this factorization in our algorithm.

**Remark.** Although Eq. (2.14) is valid for any value of $\theta \in [0, 1]$, we will use $\theta = 1/2$ (the famous Crank–Nicholson scheme). This choice of $\theta$ produces more efficient approximation [38].

## 3. Numerical results

In this section we present some numerical results of our scheme for the two-dimensional sine-Gordon equation. We use seven test problems to be able to report the results for various important cases.

### 3.1. Test problem

To observe the behavior of the numerical method, it was tested on the following problem

$$\frac{\partial^2 u}{\partial t^2} + \beta\frac{\partial u}{\partial t} = \frac{\partial^2 u}{\partial x^2} + \frac{\partial^2 u}{\partial y^2} - \sin(u), \quad -7 \le x, y \le 7, t > 0, \tag{3.1}$$

with initial conditions

$$u(x, y, 0) = 4\tan^{-1}(\exp(x + y)), \quad -7 \le x, y \le 7, t > 0, \tag{3.2}$$

$$\frac{\partial u}{\partial t}(x, y, 0) = -\frac{4\exp(x + y)}{1 + \exp(2x + 2y)}, \quad -7 \le x, y \le 7, t > 0, \tag{3.3}$$

and boundary conditions

$$\frac{\partial u}{\partial x} = \frac{4\exp(x + y + t)}{\exp(2t) + \exp(2x + 2y)}, \quad \text{for } x = -7 \text{ and } x = 7, -7 \le y \le 7, t > 0, \tag{3.4}$$

$$\frac{\partial u}{\partial y} = \frac{4\exp(x + y + t)}{\exp(2t) + \exp(2x + 2y)}, \quad \text{for } y = -7 \text{ and } y = 7, -7 \le x \le 7, t > 0. \tag{3.5}$$

Table 1

| $t$ | Explicit method | | RBF method | | |
|---|---|---|---|---|---|
| | $L_2$-error | $L_\infty$-error | $L_2$-error | $L_\infty$-error | rms |
| 1 | 0.7221 | 0.0350 | 0.2860 | 0.0670 | 0.0050 |
| 3 | 0.7877 | 0.0431 | 0.5872 | 0.0834 | 0.0103 |
| 5 | 0.5167 | 0.0404 | 0.8288 | 0.1015 | 0.0145 |
| 7 | 0.6531 | 0.0353 | 1.0706 | 0.1516 | 0.0187 |

$L_\infty$, $L_2$ errors using the explicit method and $L_\infty$, $L_2$ and rms errors using RBF method, with $\mathrm{d}t = 0.001$, $\mathrm{d}x = \mathrm{d}y = 0.25$.

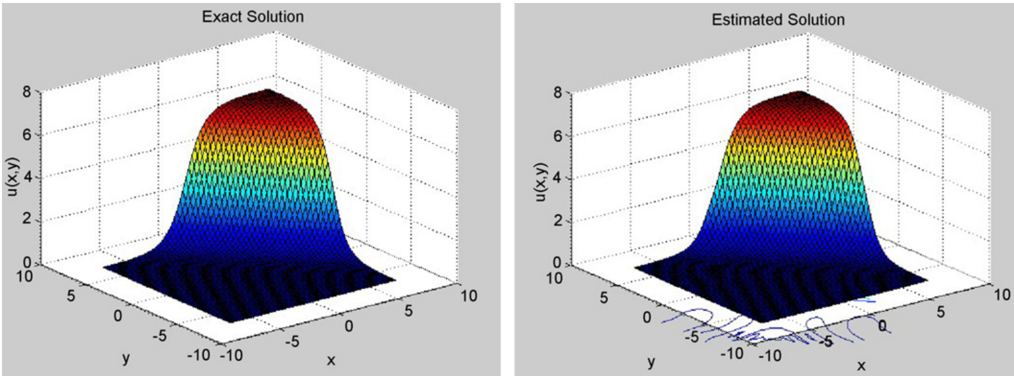


Fig. 1. Analytical and estimated solutions in $t = 7$ s, with $\mathrm{d}t = 0.001$ and $\mathrm{d}x = \mathrm{d}y = 0.25$, for test problem 3.1.

The theoretical solution of this problem, in which the parameter $\beta = 0$ is given by

$$u(x, y, t) = 4\ \tan^{-1}(\exp(x + y - t)). \tag{3.6}$$

The solution was computed for $x$ and $y$ in the intervals $-7 \leq x, y \leq 7$ and $t > 0$. The errors in the $L_2$, $L_\infty$ norms and root-mean-square (RMS) of errors at time $t = 1$, 3, 5 and 7 are given in Table 1. The first two columns in Table 1 are the error norms at different times using the explicit method used by Djidjeli et al. [14]. It can be seen from this table that the errors given by the RBF method are similar to those given by the explicit method of [14]. The graph of analytical and numerical solutions for $t = 7$ is given in Fig. 1. The absolute error of estimated solution, and the exact and estimated solutions for nodes which are accrue in line $y = x$ are given in Fig. 2.

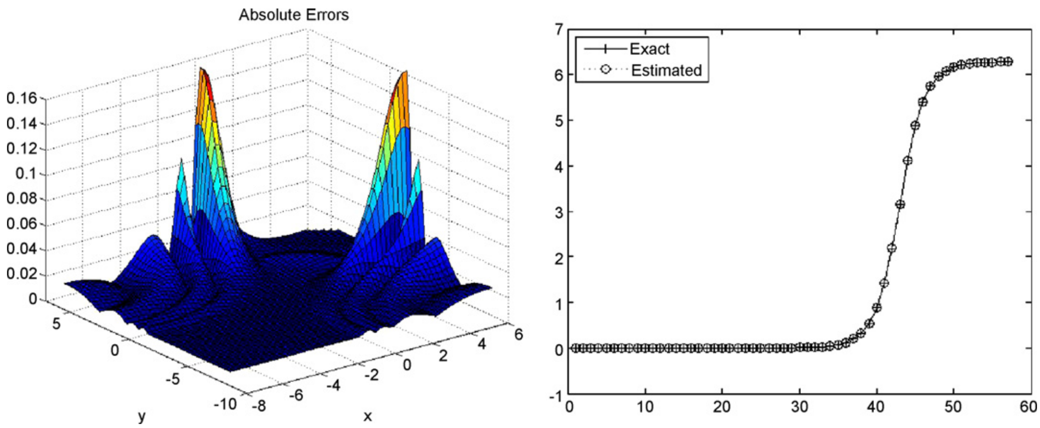


Fig. 2. (Left) absolute error of the solution, (right) analytical and estimated solutions in $t = 7$ s, with $\mathrm{d}t = 0.001$ and $\mathrm{d}x = \mathrm{d}y = 0.25$ for test problem 3.1.

By decreasing the space and the time steps, it was found that the errors have been improved in comparison with those given for $\mathrm{d}x = \mathrm{d}y = 0.25$ and $\mathrm{d}t = 0.001$, but at the cost of significantly increasing the computation time and the memory usage (one way to speed up calculations is to use the algorithms in parallel).

In the numerical calculations that follow, various cases involving line and ring solitons for the solution of (2.1) are reported; the parameter $\beta$ was given the value $\beta = 0.05$. In all the following experiments, the boundary conditions are taken to be

$$\frac{\partial u}{\partial x} = 0 \quad \text{and} \quad \frac{\partial u}{\partial y} = 0. \tag{3.7}$$

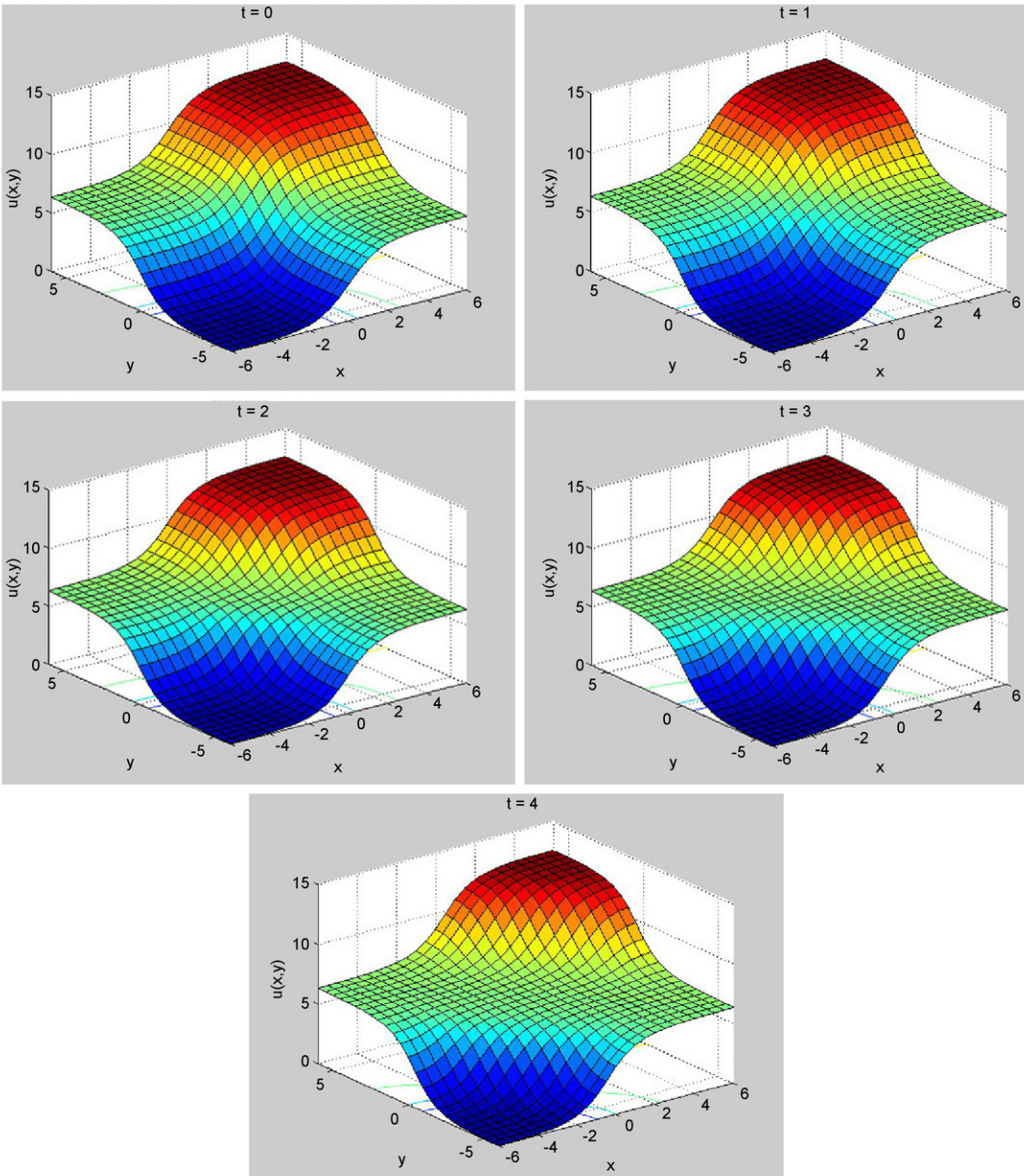


Fig. 3. Initial condition and numerical solutions at times $t = 1, 2, 3$ and 4, with $\mathrm{d}t = 0.001$ and $\mathrm{d}x = \mathrm{d}y = 0.5$, for superposition of two line solitons for test problem 3.2.

### 3.2. Superposition of two line solitons

The superposition of two line solitons is obtained for $\phi(x, y) = -1$ and initial conditions [5]

$$f(x, y) = 4\,\tan^{-1}(\exp(x)) + 4\,\tan^{-1}(\exp(y)), \quad -6 \le x, y \le 6, \tag{3.8}$$

$$g(x, y) = 0, \quad -6 \le x, y \le 6, \tag{3.9}$$

are presented in Fig. 3 for $\beta = 0.05$. The numerical solutions at times $t = 1, 2, 3$ and 4 with $\mathrm{d}t = 0.001$ and $\mathrm{d}x = \mathrm{d}y = 0.5$ are also shown. The results in Fig. 3 show the break up of two orthogonal line solitons which move away from each other undisturbed. For a small value of $\beta$, the dissipative term is found to have little effect on the superposition

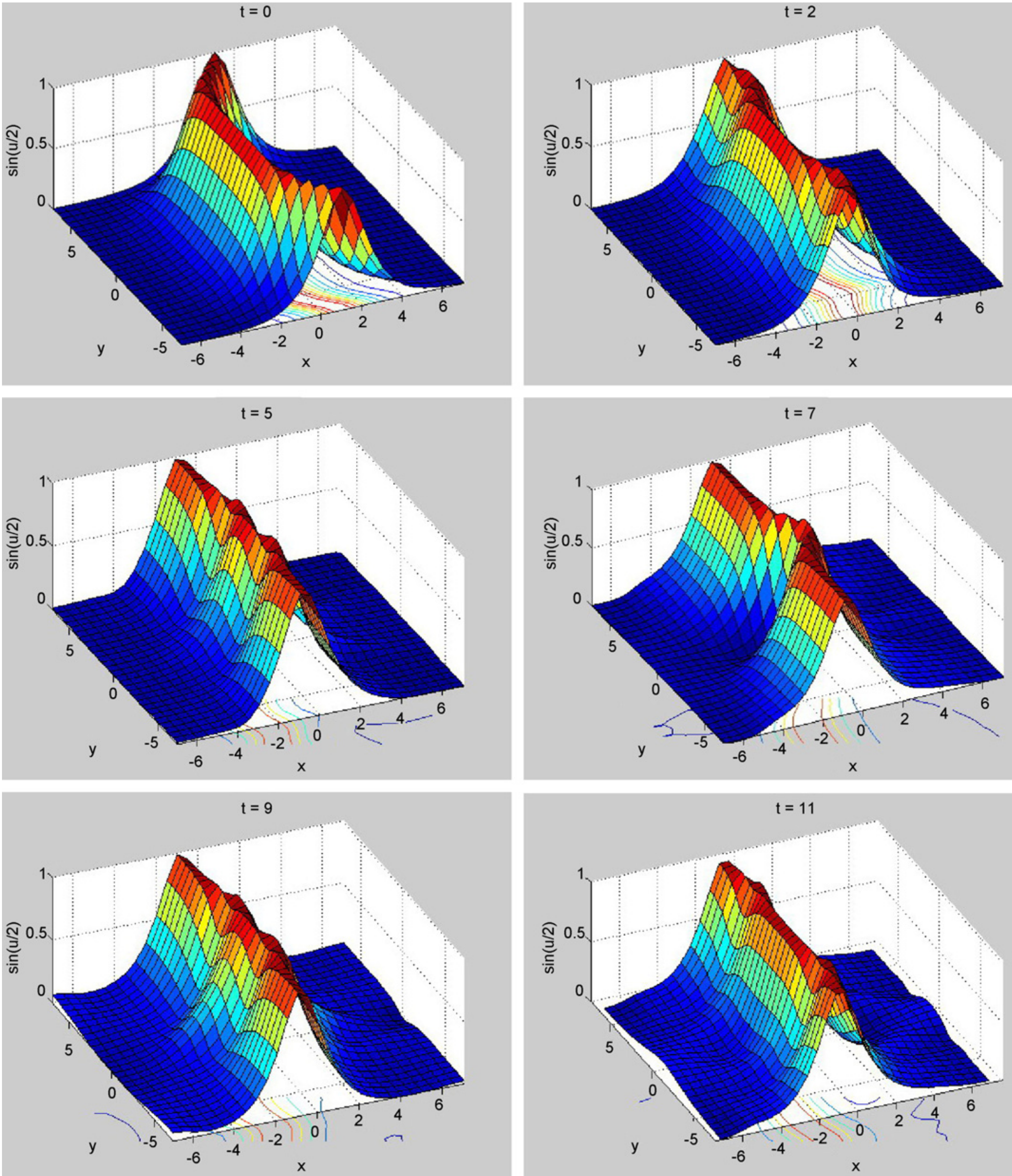


Fig. 4. Initial condition and numerical solutions at times $t = 2, 5, 7, 9$ and 11, with $\mathrm{d}t = 0.001$ and $\mathrm{d}x = \mathrm{d}y = 0.5$, for perturbation of a line soliton for test problem 3.3.

of two line solitons, although at time $t = 4$, its effect started to become visible as the moving of the break up of two orthogonal line solitons has slowed down in comparison with the undamped case. For a large value of $\beta$, however, the dissipative term is found to slow down the separation and break up of two orthogonal line solitons as time increases.

### 3.3. Perturbation of a line soliton

Perturbation of a single soliton has been depicted in Fig. 4 for $\beta = 0.05$, $dt = 0.001$ and $dx = dy = 0.5$ in terms of $\sin(u/2)$ at $t = 2, 3, 5, 7$ and 11. These results are for the case $\phi(x, y) = -1$ and initial conditions [5]

$$f(x, y) = 4 \tan^{-1}(\exp(x + 1 - 2\,\mathrm{sech}(y + 7) - 2\,\mathrm{sech}(y - 7))), \quad -7 \le x, y \le 7, \tag{3.10}$$

$$g(x, y) = 0, \quad -7 \le x, y \le 7. \tag{3.11}$$

The results show two symmetric dents moving towards each other, interacting at time $t = 7$ and after interaction the dents are seen to retain their shape after the collision. As before, a small dissipative term is found to have little effect on the symmetric perturbation of the static line solitons but a large dissipative term $\beta$ is found to slow down the formation of the dents.

### 3.4. Line soliton in an inhomogeneous medium

Numerical solutions for a line soliton in an inhomogeneous medium are obtained for the Josephson current density $\phi(x, y) = -(1 + \mathrm{sech}^2 \sqrt{x^2 + y^2})$ and the initial conditions

$$f(x, y) = 4 \tan^{-1}\left(\exp\left(\frac{x - 3.5}{0.954}\right)\right), \quad -7 \le x, y \le 7, \tag{3.12}$$

$$g(x, y) = 0.629\,\mathrm{sech}\left(\exp\left(\frac{x - 3.5}{0.954}\right)\right), \quad -7 \le x, y \le 7, \tag{3.13}$$

are presented in Fig. 5 for $\beta = 0.05$ in terms of $\sin(u/2)$ at $t = 6$, 12 and 18 with $dt = 0.001$ and $dx = dy = 0.5$ in the region $-7 \le x, y \le 7$. The results in Fig. 5 show that the line soliton is moving almost as a straight line during the transmission through inhomogeneity. For a large value of $\beta$, transmission of the line soliton across inhomogeneity was

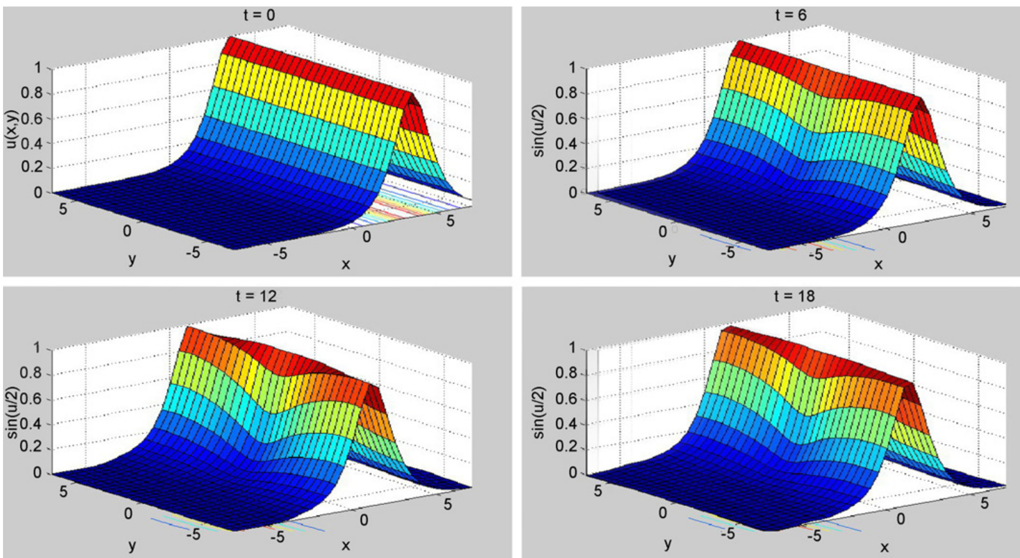


Fig. 5. Initial condition and numerical solutions at times $t = 6$, 12 and 18, with $dt = 0.001$ and $dx = dy = 0.5$, for line soliton in an inhomogeneous medium for test problem 3.4.

found to hardly move the soliton from its initial position ($t = 0$), the dissipative term is slowing down the evolution of the line soliton as time increases.

### 3.5. Circular ring soliton

Circular ring solitons are found for the case $\phi(x, y) = -1$ and initial conditions [33]

$$f(x, y) = 4\,\tan^{-1}(\exp(3 - \sqrt{x^2 + y^2})), \quad -7 \le x, y \le 7, \tag{3.14}$$

$$g(x, y) = 0, \quad -7 \le x, y \le 7. \tag{3.15}$$

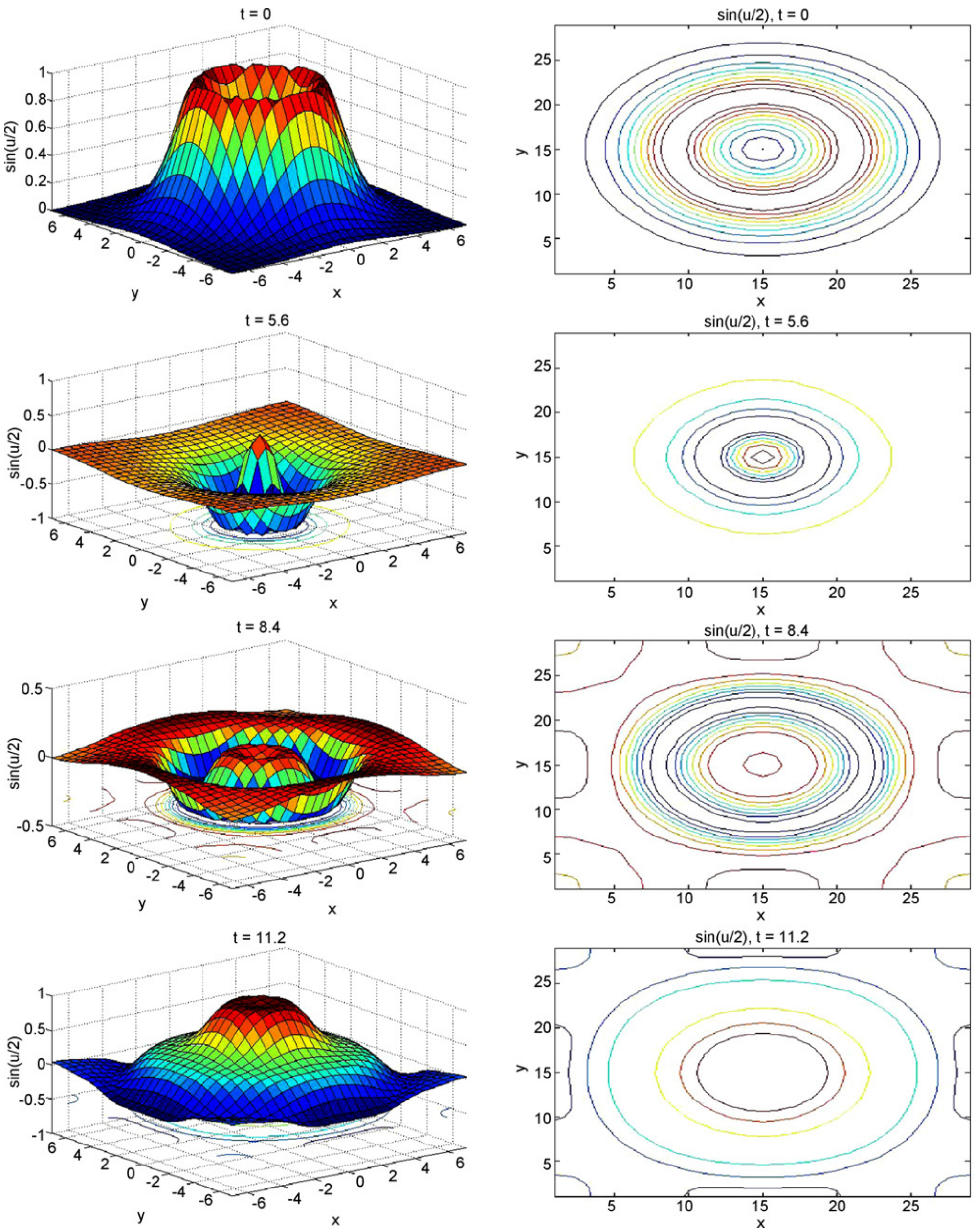


Fig. 6. Initial condition and numerical solutions at times $t = 5.6$, 8.4 and 11.2, with $\mathrm{d}t = 0.001$ and $\mathrm{d}x = \mathrm{d}y = 0.5$, for circular ring soliton for test problem 3.5.

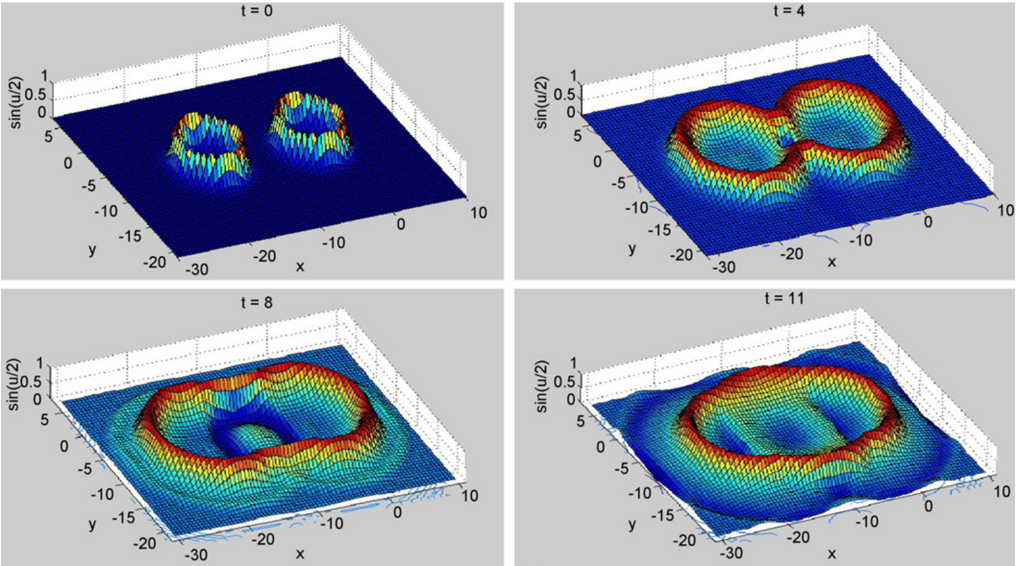


Fig. 7. Initial condition and numerical solutions at times $t = 4$, 8 and 11, with $dt = 0.001$ and $dx = dy = 0.5$, for collision of two circular ring solitons for test problem 3.6.

The solutions were sought over the domain $-7 \leq x, y \leq 7$ and are presented in Fig. 6 for $\beta = 0.05$, $dt = 0.001$ and $dx = dy = 0.5$ at $t = 2.8$, 5.6, 8.4, and 11.2 in terms of $\sin(u/2)$. At the initial stage ($t = 0$), it can be seen that the ring soliton shrinks and as time goes on, oscillations and radiations begin to form and continue to form up to $t = 8.4$. At $t = 11.2$, the graph shows that a ring soliton is nearly formed again (in the case of the damping switched off, the ring soliton was found to be already formed). For a large value of $\beta$, the initial shrunk ring soliton was found to be changing very slowly from its initial position as time increases.

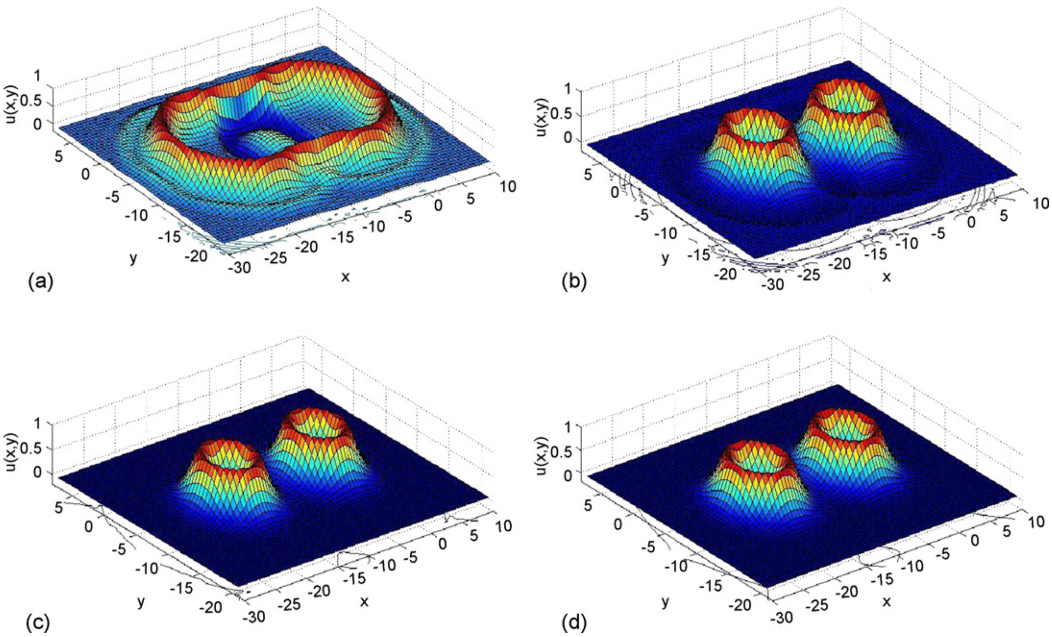


Fig. 8. Numerical solutions at time $t = 8$, with $dt = 0.001$ and $dx = dy = 0.5$, for (a) $\beta = 0.05$, (b) $\beta = 0.5$, (c) $\beta = 1.5$, and (d) $\beta = 2.5$, for collision of two circular ring solitons for test problem 3.6.

### 3.6. Collision of two circular ring solitons

The collision between two circular solitons is considered for $\phi(x, y) = -1$ and initial conditions [33]

$$f(x, y) = 4\ \tan^{-1}\left(\exp\left(\frac{4-\sqrt{(x+3)^2+(y+7)^2}}{0.436}\right)\right), \quad -10 \le x \le 10, -7 \le y \le 7, \tag{3.16}$$

$$g(x, y) = 4.13\,\mathrm{sech}\left(\exp\left(\frac{4-\sqrt{(x+3)^2+(y+7)^2}}{0.436}\right)\right), \quad -10 \le x \le 10, -7 \le y \le 7, \tag{3.17}$$

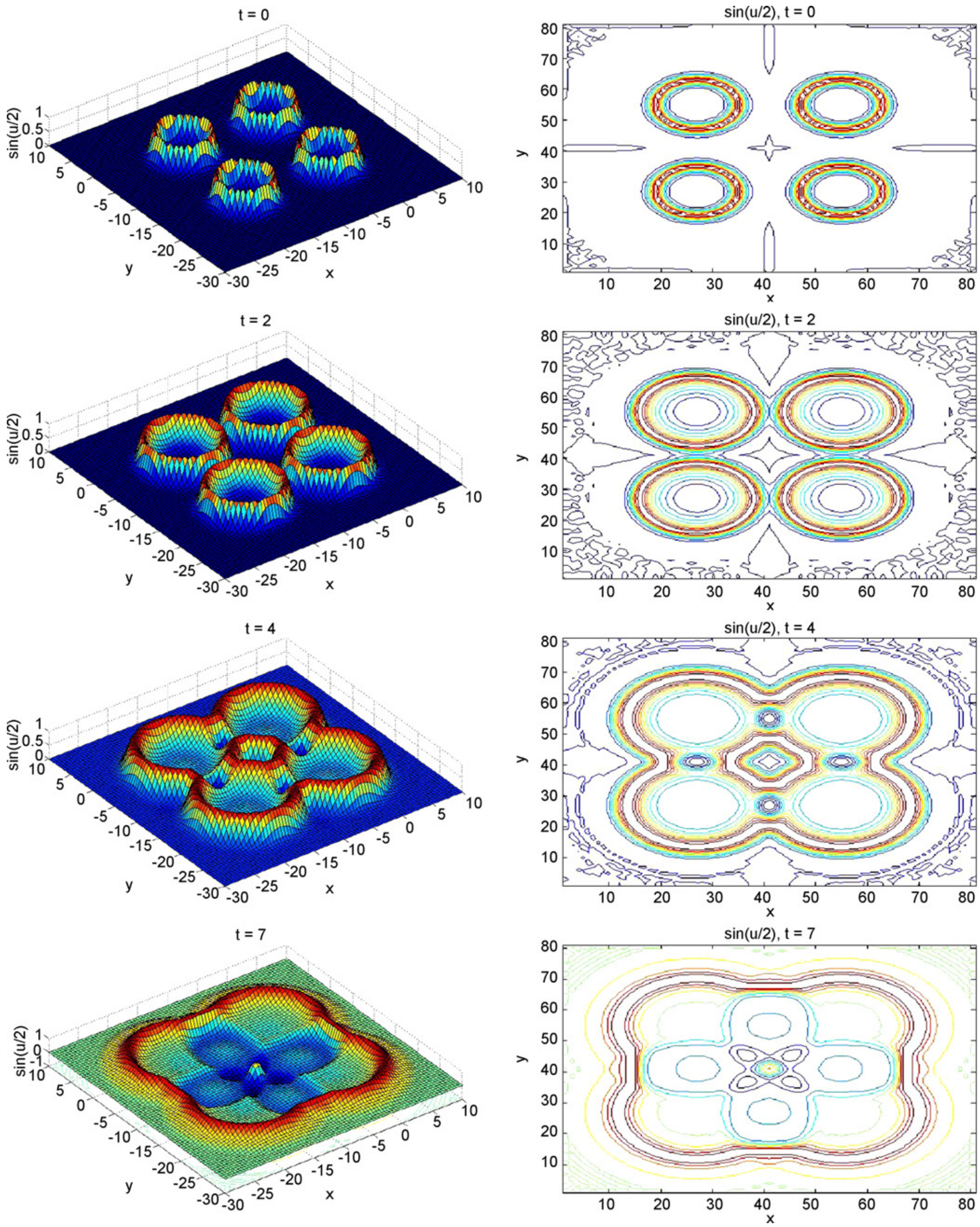


Fig. 9. Initial condition and numerical solutions at times $t = 2$, 4 and 7, with $dt = 0.001$ and $dx = dy = 0.5$, for collision of four circular ring solitons for test problem 3.7.

over the region $-10 \le x \le 10$, $-7 \le y \le 7$ and are presented in Fig. 7 for $\beta = 0.05$, $\mathrm{d}t = 0.001$ and $\mathrm{d}x = \mathrm{d}y = 0.5$ at $t = 4$, 8 and 11 in terms of $\sin(u/2)$. The solution is extended across $x = -10$ and $y = -7$ by symmetry relations. The results in Fig. 7 show the collision between two expanding circular ring solitons in which, as a result of the collision, two oval ring solitons bounding an annular region emerge into a larger oval ring soliton. For a large value of $\beta$, it is found that the dissipative term is slowing down the two initial ring solitons to emerge into a larger oval ring soliton. For example, with $\beta = 5$ the two ring solitons at time $t = 11$ still look like those given at $t = 1.5$ for $\beta = 0.05$. For see this, we draw the numerical solution at $t = 8$ for $\beta = 0.05$, 0.5, 1.5, and 2.5 in Fig. 8.

### 3.7. Collision of four circular ring solitons

Finally, a collision of four expanding circular ring solitons is investigated for $\phi(x, y) = -1$ and initial conditions [33]

$$f(x, y) = 4 \tan^{-1}\left(\exp\left(\frac{4 - \sqrt{(x+3)^2 + (y+3)^2}}{0.436}\right)\right), \tag{3.18}$$

$$g(x, y) = \frac{4.13}{\cosh(\exp((4 - \sqrt{(x+3)^2 + (y+3)^2})/0.436))}, \tag{3.19}$$

over the domain $-10 \le x, y \le 10$. The solution was found over one-quarter of the domain and then it was extended across $x = -10$ and $y = -10$ by symmetry relations. The results are depicted in Fig. 9. for $\beta = 0.05$, $\mathrm{d}t = 0.001$ and $\mathrm{d}x = \mathrm{d}y = 0.5$ at $t = 2$, 4 and 7 in terms of $\sin(u/2)$, from which observations similar to those related to the collision of two expanding circular ring solitons may be made.

## 4. Conclusion

A RBF-based numerical method proposed for the solution of the nonlinear sine-Gordon equation and tested in a variety of calculations where it showed superior performance. The numerical method uses collocation points and approximates the solution using thin plate splines (TPS) radial basis function (RBF). The scheme works in a similar fashion as finite difference methods. By decreasing the space and the time steps, it was found that the errors have been improved, but at the cost of significantly increasing the computation time and the memory usage. Finally, it was seen that, for the case where the exact solution is known, the numerical results demonstrate the good accuracy of this scheme. These results supported the confidence in applying this method to problem (2.1) in which the theoretical solution is not known. A meshfree method does not require a mesh to discretize the domain of the problem under consideration, and the approximate solution is constructed entirely based on a set of scattered nodes. This method does not require mesh generation which makes them advantageous for three-dimensional problems as well as problems that require frequent re-meshing such as those arising in nonlinear analysis. Due to its simplicity to implement, it represents an attractive alternative to the finite-difference method and the finite-element method as a solution method of nonlinear differential equations. The main idea behind the new approach can be investigated to solve the partial differential equations studied in [42–45].

## Acknowledgments

The authors thank the anonymous reviewers for the constructive comments and suggestions.

## References

[1] S.G. Ahmed, A collocation method using new combined radial basis functions of thin plate and multiquadraic types, Eng. Anal. Bound. Elem. 30 (2006) 697–701.
[2] J. Argyris, M. Haase, An engineer's guide to soliton phenomena, Application of the finite element method, Comput. Methods Appl. Mech. Eng. 61 (1987) 71–122.
[3] J. Argyris, M. Haase, J.C. Heinrich, Finite element approximation to two-dimensional sine-Gordon solitons, Comput. Methods Appl. Mech. Eng. 86 (1991) 1–26.
[4] A.G. Bratsos, A third order numerical scheme for the two-dimensional sine-Gordon equation, Math. Comput. Simulation 76 (2007) 271–282.

[5] A.G. Bratsos, The solution of the two-dimensional sine-Gordon equation using the method of lines, J. Comput. Appl. Math. 206 (2007) 251–277.
[6] A.G. Bratsos, An explicit numerical scheme for the sine-Gordon equation in 2 + 1 dimensions, Appl. Numer. Anal. Comput. Math. 2 (2) (2005) 189–211.
[7] A.G. Bratsos, A modified predictor-corrector scheme for the two-dimensional sine-Gordon equation, Numer. Algor. 43 (2006) 295–308.
[8] J.T. Chen, I.L. Chen, K.H. Chen, Y.T. Lee, Y.T. Yeh, A meshless method for free vibration analysis of circular and rectangular clamped plates using radial basis function, Eng. Anal. Bound. Elem. 28 (5) (2004) 535–545.
[9] P.L. Christiansen, P.S. Lomdahl, Numerical solution of 2 + 1 dimensional sine-Gordon solitons, Physica 2D (1981) 482–494.
[10] P.L. Christiansen, O.H. Olsen, On dynamical two-dimensional solutions to the sine-Gordon equation, Z. Angew. Math. Mech. 59 (30) (1979) 10.
[11] M. Dehghan, Finite difference procedures for solving a problem arising in modeling and design of certain optoelectronic devices, Math. Comput. Simulation 71 (2006) 16–30.
[12] M. Dehghan, A. Shokri, A numerical method for KdV equation using collocation and radial basis functions, Nonlinear Dyn. 50 (2007) 111–120.
[13] M. Dehghan, D. Mirzaei, The dual reciprocity boundary element method (DRBEM) for two-dimensional sine-Gordon equation, Comput. Methods Appl. Mech. Eng. 197 (2008) 476–486.
[14] K. Djidjeli, W.G. Price, E.H. Twizell, Numerical solutions of a damped sine-Gordon equation in two space variables, J. Eng. Math. 29 (1995) 347–369.
[15] C. Franke, R. Schaback, Convergence orders of meshless collocation methods using radial basis functions, Adv. Comput. Math. 8 (4) (1997) 381–399.
[16] C. Franke, R. Schaback, Solving partial differential equations by collocation using radial basis functions, Appl. Math. Comput. 93 (1) (1998) 73–82.
[17] C. Gorria, Yu.B. Gaididei, M.P. Soerensen, P.L. Christiansen, J.G. Caputo, Kink propagation and trapping in a two-dimensional curved Josephson junction, Phys. Rev. B 69 (2004) 1–10.
[18] B.-Y. Guo, P.J. Pascual, M.J. Rodriguez, L. Vzquez, Numerical solution of the sine-Gordon equation, Appl. Math. Comput. 18 (1986) 1–14.
[19] R.L. Hardy, Multiquadric equations of topography and other irregular surfaces, Geophys. Res. 176 (1971) 1905–1915.
[20] M.A. Helal, Soliton solution of some nonlinear partial differential equations and its application in fluid mechanics, Chaos Solitons Fractals 13 (2002) 1917–1929.
[21] R. Hirota, Exact three-soliton solution of the two-dimensional sine-Gordon equation, J. Phys. Soc. Jpn. 35 (1973) 15–66.
[22] Y.C. Hon, Z. Wu, Additive Schwarz domain decomposition with radial basis approximation, Int. J. Appl. Math. 4 (1) (2000) 599–606.
[23] J.D. Josephson, Supercurrents through barriers, Adv. Phys. 14 (1965) 419–451.
[24] P. Kaliappan, M. Lakshmanan, Kadomtsev-Petviashvili and two-dimensional sine-Gordon equations: reduction to Painlev transcendents, J. Phys. A: Math. Gen. 249 (1979) 23.
[25] E.J. Kansa, Multiquadrics—a scattered data approximation scheme with applications to computational fluid dynamics. I, Comput. Math. Appl. 19 (1990) 127–145.
[26] E.J. Kansa, Multiquadrics—a scattered data approximation scheme with applications to computational fluid dynamics. II, Comput. Math. Appl. 19 (1990) 147–161.
[27] D.J. Kaup, A.C. Newell, Solitons as particles, oscillators, and in slowly changing media: a singular perturbation theory, Proc. Roy. Soc. London Ser. A 361 (1978) 413–446.
[28] K.L. Liew, Mesh-free radial basis function method for buckling analysis of non-uniformly loaded arbitrarily shaped shear deformable plates, Comput. Methods Appl. Mech. Eng. 193 (3) (2004) 205–224.
[29] W.R. Madych, S.A. Nelson, Multivariate interpolation and conditionally positive definite functions II, Math. Comput. 54 (189) (1990) 211–230.
[30] W.R. Madych, S.A. Nelson, Bounds on multivariate polynomials and exponential error estimates for multiquadric interpolation, J. Approx. Theory 70 (1992) 94–114.
[31] K. Nakajima, Y. Onodera, T. Nakamura, R. Sato, Numerical analysis of vortex motion on Josephson structures, J. Appl. Phys. 45 (9) (1974) 4095–4099.
[32] D. Nardini, C.A. Brebbia, A New Approach to Free Vibration Analysis Using Boundary Elements, Boundary Element Methods in Engineering, Computational Mechanics Publications, Southampton, 1982.
[33] Q. Sheng, A.Q.M. Khaliq, D.A. Voss, Numerical simulation of two-dimensional sine-Gordon solitons via a split cosine scheme, Math. Comput. Simulation 68 (2005) 355–373.
[34] M. Vitor, RBF-based meshless methods for 2D elastostatic problems, Eng. Anal. Bound. Elem. 28 (10) (2004) 1271–1281.
[35] H. Wendland, Piecewise polynomial, positive definite and compactly supported radial functions of minimal degree, Adv. Comput. Math. 4 (1995) 389–396.
[36] J.X. Xin, Modeling light bullets with the two-dimensional sine-Gordon equation, Physica D 135 (2000) 345–368.
[37] J. Zagrodzinsky, Particular solutions of the sine-Gordon equation in 2 + 1 dimensions, Phys. Lett. 72A (1979) 284–286.
[38] M. Zerroukat, H. Power, C.S. Chen, A numerical method for heat transfer problem using collocation and radial basis functions, Int. J. Numer. Methods Eng. 42 (1992) 1263–1278.
[39] M. Dehghan, On the solution of an initial-boundary value problem that combines Neumann and integral condition for the wave equation, Numer. Methods Partial Differ. Equations 21 (2005) 24–40.
[40] M. Dehghan, Parameter determination in a partial differential equation from the overspecified data, Math. Comput. Model. 41 (2005) 196–213.
[41] M. Dehghan, The one-dimensional heat equation subject to a boundary integral specification, Chaos, Solitons Fractals 32 (2007) 661–675.
[42] M. Dehghan, Implicit collocation technique for heat equation with non-classic initial condition, Int. J. Nonlin. Sci. Numer. Simul. 7 (2006) 447–450.

[43] M. Dehghan, A computational study of the one-dimensional parabolic equation subject to nonclassical boundary specifications, Numer. Methods Partial Differ. Equations 22 (2006) 220–257.

[44] F. Shakeri, M. Dehghan, Numerical solution of the Klein-Gordon equation via He's variational iteration method, Nonlin. Dynam. 51 (2008) 89–97.

[45] M. Dehghan, F. Shakeri, Application of He's variational iteration method for solving the Cauchy reaction–diffusion problem J. Comput. Appl. Math. 214 (2008) 435–446.